

# Performance Analysis of Periodic Cellular-IoT Communication with Immediate Release of Radio Resources

Shuya Abe

*Graduate School of  
Information Science and Technology  
Osaka University  
1-5 Yamadaoka, Suita,  
Osaka 565-0871, Japan  
Email: s-abe@ist.osaka-u.ac.jp*

Go Hasegawa

*Research Institute of Electrical Communication  
Tohoku University  
2-1-1 Katahira, Aoba-ku,  
Sendai 980-8577, Japan  
Email: hasegawa@riec.tohoku.ac.jp*

Masayuki Murata

*Graduate School of  
Information Science and Technology  
Osaka University  
1-5 Yamadaoka, Suita,  
Osaka 565-0871, Japan  
Email: murata@ist.osaka-u.ac.jp*

**Abstract**—Mobile cellular networks are now serving all kinds of Internet of Things (IoT) communications. Since current contention-based random access and radio resource allocation are optimized for traditional human communications, massive IoT communications cannot be efficiently accommodated. For this reason, standardization activities for connecting IoT devices, such as Cellular-IoT (C-IoT), have emerged. However, there have been few studies devoted to the evaluation of the performance of the C-IoT communications with periodic data transmissions, despite their being the common characteristics of many IoT communications.

Herein, we evaluate the capacity of mobile cellular networks in accommodating periodic C-IoT communications, focusing on differences in performance between LTE and Narrowband-IoT (NB-IoT) networks. To achieve this, we conduct end-to-end performance analyses of both control and data planes, including the random access procedure, radio resource allocation, and bearer establishment in EPC network. Moreover, we determined the effect of immediate release of radio resources considered in 3GPP. Numerical evaluation results show that NB-IoT can accommodate more IoT devices than LTE, although this results in significant latency in data transmission. Furthermore, we find that the number of IoT devices that can be accommodated increases up to 20.7 times with immediate release of radio resources.

**Index Terms**—Cellular Internet of Things (C-IoT), narrowband IoT (NB-IoT), Radio Access Network, Mobile core networks

## I. INTRODUCTION

Traditionally, mobile networks only accommodate human devices, such as smartphones, however, they are now also serving numerous Internet of Things (IoT) communications. Because the current control- and data-plane mechanisms of mobile cellular networks, such as contention-based random access, radio resource allocation, and bearer establishment procedure, are predominantly optimized for human communications, IoT communications cannot generally be efficiently accommodated. IoT traffic has different characteristics from human communications. In particular, the Third-Generation Partnership Project (3GPP) assumes that most cellular IoT traffic results from periodic data transmissions of Mobile

Autonomous Reporting (MAR) such as sensors and smart meters [1], [2]. In [1], the 3GPP presents a typical example of an inter-arrival time distribution for MAR: 1 day (40%), 2 hours (40%), 1 hour (15%), and 30 minutes (5%).

For this reason, standardization activities for connecting IoT devices to cellular networks, such as Cellular-IoT (C-IoT), have emerged. C-IoT can be deployed over an existing infrastructure, and is advantageous in terms of maintaining security and managing radio interference. Among C-IoT radio technologies, Narrowband-IoT (NB-IoT) is optimized for most IoT communications that transmit small data. Moreover, in standardization activities, the immediate release of radio resources after the completion of data transmissions is considered [3], [4], whereas radio resources are kept allocated at least 10 seconds in traditional mobile cellular networks. The immediate release of radio resources would have a considerable effect in accommodating IoT communications with small data transmissions.

In order to improve the capacity of mobile cellular networks for IoT communications, various methods have been proposed. Previous studies [4], [5] have focused on accommodating periodic data transmissions in the mobile cellular network. In [4], power consumption with the application of immediate release of radio resources was studied, however, the authors did not consider the collisions of preamble transmissions and radio resource allocation. The authors of [5] evaluated both the collision of preamble transmissions and radio resource allocation, however, the immediate release of radio resources was beyond the scope of the work. [6] compared the performance of NB-IoT with Long Term Evolution (LTE) while considering various data sizes. The authors of [7] evaluated the effect of collisions between preamble transmissions in detail with numerical analysis or simulation. In summary, few existing studies have evaluated the performance of C-IoT communications with periodic data transmissions in terms of the immediate release of radio resources.

The main contributions of this paper are therefore an analy-

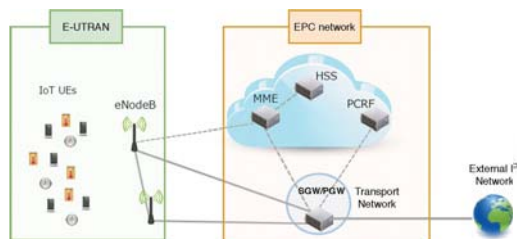


Fig. 1: Mobile core network architecture.

sis of the performance of periodic C-IoT communications, and a numerical evaluation of the effect of immediate release of radio resources. We show the mathematical analysis of both data- and control- plane performance, including random access procedures, radio resource allocation, bearer establishment, and user-data transmission. We adopted a two-dimensional Markov chain model to analyze the behavior of User Equipments (UEs) in a random access procedure. We also exploited queuing theory for the derivation of the failure probability of radio resource allocation and the time required for bearer establishment. We give numerical evaluation results of these analyses in order to compare the performance of the LTE and NB-IoT networks, in addition to the effect of immediate release of radio resources.

## II. NETWORK MODEL

The mobile network architecture is shown in Fig. 1. It consists of two networks, an evolved universal terrestrial radio access network (E-UTRAN) and EPC. We assume that when the UE transmits data, it first conducts a random access procedure in order to obtain radio resources. Following this, a bearer establishment procedure is executed to set up bearers for the UE, which are the logical transmission paths in the data plane. Finally, the UE sends the user data.

### A. Random Access Procedure and Radio Resource Allocation in E-UTRAN

E-UTRAN consists of user equipments (UEs) and eNodeBs. An eNodeB implements a remote radio head and accommodates multiple IoT UEs, which transmit data periodically. We assume that all UEs transmit data of the same size with identical periodic interval.

When the UE starts data transmission, it conducts a contention-based random access, termed the Radio Resource Control (RRC) connection setup procedure, in both the LTE and NB-IoT [8], [9]. This process consists of the following four steps:

- 1) The UE transmits a preamble to the eNodeB, which is randomly selected from multiple preambles reserved in the cell. The number of preambles is 54 in LTE and 48 in NB-IoT.
- 2) When the eNodeB receives the preamble, it transmits a Random Access Channel (RACH) response message to the corresponding UE.

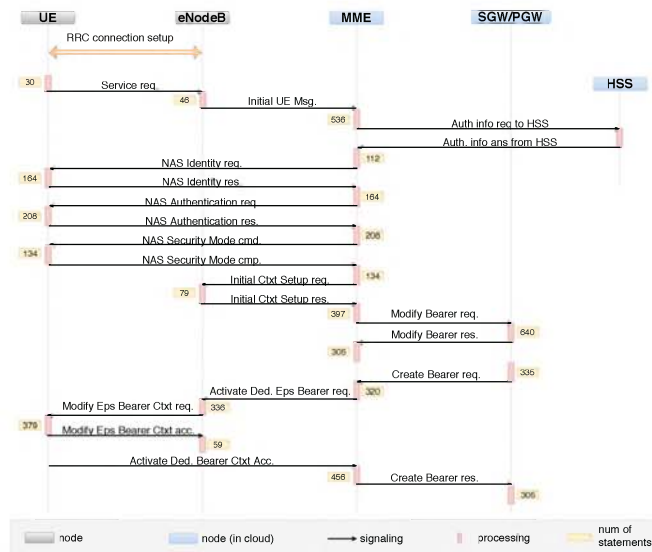


Fig. 2: Signaling flow for bearer establishment.

- 3) The UE that has received the RACH response message sends an RRC connection request message to the eNodeB. This request message contains the identity of the UE.
- 4) After receiving the RRC connection request message, the eNodeB transmits an RRC connection setup message to the UE that includes cell setting information.

When the UE receives the RRC connection setup message including its identity, the random access procedure has successfully finished. If this does not occur, the random access has failed and the procedure is performed again after a back off time.

When the UE completes the RRC connection setup, radio resources are allocated to the UE. Radio resources and RRC connections are allocated until the inactivity timer expires. The typical value of an inactivity timer is 10 [s] [10]. In 3GPP, the immediate release of radio resources after data transmissions is considered [9], such that the radio resource and RRC connection are immediately released when the UE concludes data transmission. It would be effective to have IoT communications with small data transmissions. Such a possibility is evaluated in this paper.

### B. Bearer Establishment Procedure in EPC

As shown in Fig. 1, EPC consists of a serving gateway/packet data network gateway (SGW/PGW), a mobile management entity (MME), a home subscriber server (HSS), and a policy and charging rules function (PCRF). Fig. 2 shows the signaling flow when a UE changes its state from idle to active and sends a communication request after the RRC connection setup. In this figure, req. and res. represent a request and a response message, respectively. Msg. stands for “message”. Ctxt, Ded., and Acc mean “Context”, “Dedicated”, and “Accept”, respectively. The figure includes the number of statements executed by each EPC node for processing each

signaling message in the programs. This number is obtained by analyzing the source code of OpenAirInterface [11]. Note that each processing of signaling messages has a different number of statements, meaning that each message imposes a different load on the corresponding EPC node.

### III. ANALYSIS

We give analytical results for the average of *service time*, which is defined as the time between the moment at which the a UE starts a random access procedure and when it completes a bearer establishment procedure and data transmission. The service time  $t_{service}$  is the sum of *random access time*  $t_r$ , *bearer establishment time*  $t_b$  and *data transmission time*  $t_d$ , as presented (1).

$$t_{service} = t_r + t_b + t_d \quad (1)$$

#### A. Random Access Time

As explained in Subsection II-A, when the UE starts a random access procedure, it transmits a preamble, and radio resource allocation is performed if no collision has occurred in the preamble transmission. After data transmission with the allocated radio resource, the UE waits for the next communication timing. On the other hand, when a collision occurs in the preamble transmission or when the radio resource allocation fails, the UE restarts preamble transmission after waiting for a *MAC-level back off* whose length is randomly determined within a range of up to  $B_M$  [slots]. Note that the length of a slot is equal to 0.5 [ms] in both LTE and NB-IoT [9]. This procedure is repeated up to  $N_M - 1$  times until both the preamble transmission and radio resource allocation have been successfully completed. In this paper, we also consider the *application-level back off* after  $N_M - 1$  times of MAC-level back off. For simplicity, the length of the application back off is fixed at  $B_A$  [slots].

1) *State Transition Diagram*: We exploit a two dimensional Markov chain to model the above-described behavior of a UE, depicted in Fig. 3. This is based on the models in [7], [12], which we have extended to include MAC-level back off, application-level back off, and wait time after data transmission for periodic communications. All state transitions take 1 [slot]. In Fig. 3,  $T_c$  is the data transmission cycle of UEs.  $B_M$  [slots] is the maximum time for the MAC-level back off.  $B_A$  [slots] is the time for the application-level back off.  $p_f$  is the probability that the preamble transmission collides or succeeds without collision but the radio resource allocation fails nonetheless.  $p_{i,j}$  represents the probability of transition from state  $(i-1, 0)$  to state  $(i, j)$ . No description of transition probability indicates that the transition probability is 1.0. We assume that data transmission is completed prior to beginning the transmission of the next cycle. Therefore, we consider that  $T_c \geq t_r$  is always satisfied.

When a UE is in states such as  $(1, 0), \dots, (N_M, 0)$ , depicted in orange ellipses in Fig. 3, the UE transmits a preamble. When the preamble transmission and radio resources allocation have been conducted successfully, the UE waits for the next data transmission, depicted by blue arrows. On the

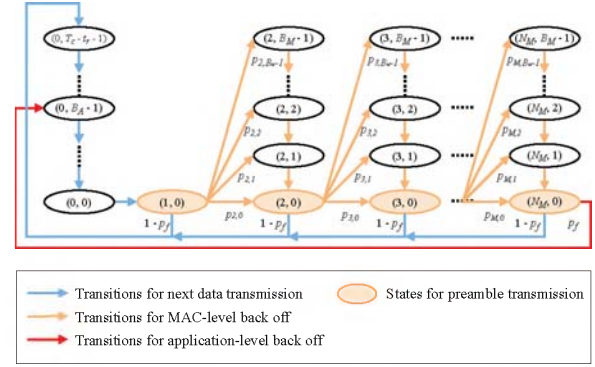


Fig. 3: State transition diagram for random access procedure

other hand, when the UE fails the preamble transmission or radio resources allocation, it begins the MAC-level back off, depicted by orange arrows. When these failures are repeated  $N_M$  times, an application-level back off occurs, depicted by a red arrow.

By calculating the probability of the UE being in each state, defined as the state probability, we obtain the average time required for the random access procedure. According to Fig. 3, when the probability of state  $(i, j)$  is denoted by  $\pi_{(i,j)}$ , the following equations are satisfied for  $i = 0, 1, \dots, (T_c - t_r - 1)$ ,  $j = 2, 3, \dots, N_M$ , and  $k = 0, 1, \dots, (B_M - 1)$ .

$$\pi_{(0,i)} = \pi_{(0,0)} \quad (2)$$

$$\pi_{(1,0)} = \pi_{(0,0)} \quad (3)$$

$$\begin{aligned} \pi_{(j,k)} &= \sum_{i=k}^{B_M-1} \pi_{(j-1,0)} p_{j,i} \\ &= \frac{B_M - k}{B_M} p_f^{j-1} \pi_{(0,0)} \end{aligned} \quad (4)$$

Since the sum of the probabilities of all states must equal 1.0, the following equation is satisfied:

$$\sum_{i=0}^{T_c - t_r - 1} \pi_{(0,i)} + \pi_{(1,0)} + \sum_{j=2}^{N_M} \sum_{k=0}^{B_M-1} \pi_{(j,k)} = 1 \quad (5)$$

According to (2)–(5), the state probability of the initial state  $(0,0)$  is derived by (6).

$$\pi_{(0,0)} = \frac{2(1 - p_f)}{2(T_c - t_r + 1)(1 - p_f) + (B_M + 1)p_f(1 - p_f^{N_M-1})} \quad (6)$$

In order to calculate the state probabilities, it is necessary to obtain  $p_f$  and  $t_r$ ; these are not given as system parameters.  $p_f$  is derived using (7), where  $p_c$  is the collision probability of the preamble transmission and  $p_r$  is the failure probability of the radio resource allocation.

$$p_f = 1 - (1 - p_c)(1 - p_r) \quad (7)$$

$p_c$  and  $p_r$  are given below. In order to calculate  $t_r$ , we consider the detailed behavior of MAC- and application-level back offs. Since an application-level back off occurs after a MAC-level

back off is repeated  $(N_M - 1)$  times,  $t_r$  is given by the following equations, where  $t_M$  is the average time for MAC-level back offs with successful preamble transmission, and  $t_A$  is the average time for an application-level back off with  $(N_M - 1)$  times of MAC-level back offs.

$$t_r = \sum_{k=1}^{n_A} (p_f^{N_M})^{k-1} ((k-1)t_A + t_M) \quad (8)$$

$$t_M = 1 + \frac{B_M + 1}{2} \sum_{i=1}^{N_M-1} p_f^i \quad (9)$$

$$t_A = 1 + \frac{B_M + 1}{2} (N_M - 1) + B_A \quad (10)$$

2) *Preamble Transmission Probability*: In this study, we assume that when two or more UEs transmits the same preamble at the same time, a collision occurs and that all colliding preamble transmissions fail. In this case, the UEs perform MAC-level back off.

Therefore,  $p_c$ , i.e., the collision probability of preamble transmission, can be obtained using (11), where  $n_U$  is the number of UEs accommodated in the eNodeB,  $P$  is the number of preambles and  $p_t$  is the probability at which the UE is in a state of preamble transmission.

$$p_c = 1 - \left( \frac{P-1}{P} \right)^{(n_U-1)p_t} \quad (11)$$

According to Fig. 3,  $p_t$  is derived by (12).

$$p_t = \sum_{i=1}^{N_M} \pi_{(i,0)} \quad (12)$$

With (4) and (6), this equation can be expanded as follows.

$$p_t = \frac{2(1 - p_f^{N_M})}{2(T_c - t_r + 1)(1 - p_f) + (B_M + 1)p_f(1 - p_f^{N_M-1})} \quad (13)$$

3) *Radio Resource Allocation*: Even when a UE succeeds in preamble transmission, data transmission can be made only when radio resource allocation has been successfully conducted, otherwise, the UE goes into a MAC-level back off.

The number of resource blocks in LTE and NB-IoT with a given radio bandwidth is denoted by  $n_R$ . For simplicity, it is assumed that the number of resource blocks allocated to each UE is fixed at  $n_{RU}$ . The maximum number of UEs to which the network can concurrently allocate the radio resource is then  $\lfloor \frac{n_R}{n_{RU}} \rfloor$ . We also assume that the radio resource is kept allocated until the inactivity timer expires. Furthermore, for simplicity, we assume that a Poisson arrival process of UEs that successfully transmit their preambles. We then employ the  $M/D/K/K$  queuing model [13] to derive the failure probability for radio resource allocation. In the  $M/D/K/K$

model, the steady-state distribution of the number of jobs in a system is represented by (14),

$$P(L = n) = \frac{(\lambda\tau)^n}{n!} \sum_{i=0}^K \frac{(\lambda\tau)^i}{i!} \quad (0 \leq n \leq K) \quad (14)$$

where  $\lambda$  is the job arrival rate,  $\tau$  is the serving time,  $K$  is the number of servers, and  $L$  is the number of jobs in the system. In our model,  $P(L = K)$  corresponds to the failure probability of radio resource allocation,  $p_r$ , which has the following parameter calculations:

$$\lambda = n_s n_U p_t (1 - p_c) \quad (15)$$

$$\tau = T_i \quad (16)$$

$$K = \left\lfloor \frac{n_R}{n_{RU}} \right\rfloor \quad (17)$$

where  $n_s$  is the number of slots per second and  $T_i$  is the inactivity timer discussed in Subsubsection III-A3. When we employ the immediate release of radio resources, we set the value of  $T_i$  to  $t_{service}$ . This means that  $t_{service}$  and  $p_r$  are dependent upon one another. Therefore, when obtaining numerical results, we make iterations for the calculation of  $t_{service}$  and  $p_r$  until both values converge.

### B. Bearer Establishment Time

Based on the signalling flow in Fig. 2, the bearer establishment time  $t_b$  is the sum of the propagation delays of all signaling messages, denoted by  $t_\tau$ , and the processing times of all messages, denoted by  $t_t$ .

$$t_b = t_\tau + t_t \quad (18)$$

In this paper, we use the analysis results of the bearer establishment time in our previous study [14], while we modify the calculation of the average processing time.

To derive the average processing time at a mobile core node, we employ the M/G/1/PS queuing model [15] and assume that the arrival of signaling messages at a node follows a Poisson distribution. In the M/G/1/PS model, the mean sojourn time  $E[R]$  can be derived as follows (19):

$$E[R] = \frac{\rho^r}{1 - \rho} \frac{E[S^2]}{2E[S]} + \frac{1 - \rho^r}{1 - \rho} E[S] \quad (19)$$

where  $\lambda$  is job arrival rate,  $S(x)$  is workload distribution,  $E[S]$  is the mean workload, and  $r$  is the maximum number of parallel processing runs.  $\rho$  is the system utilization, and is given by the following equation.

$$\rho = \lambda E[S] \quad (20)$$

In our analysis, a job to be processed at a server corresponds to a signaling message to be processed at a mobile core node. The workload of each job corresponds to the number of statements in the program executed at the mobile core node for processing the signaling message, and this is presented numerically in Fig. 2. The job arrival rate at node  $N$ , denoted by  $\lambda_N$ , corresponds to the number of signaling messages

arriving per unit time at node  $N$ . Note that the jobs for the bearer establishment arrive only from UEs that successfully finish the preamble transmission and radio resource allocation. Consequently, the time distribution for processing signaling messages at node  $N$ , denoted by  $S_N$ , corresponds to the distribution of the workload. Accordingly, the mean workload  $E[S_N]$  can be calculated on the basis of the average number of statements for processing signaling messages and the server resource of node  $N$ .  $\lambda_N$ ,  $E[S_N]$ , and  $E[S_N^2]$  may therefore be derived as (21)–(23),

$$\lambda_N = \frac{P_N n_U n_E (1 - p_f) p_t}{T_c} \quad (21)$$

$$E[S_N] = \sum_{i=1}^{P_N} \frac{L_{N_i}}{R_N P_N} \quad (22)$$

$$E[S_N^2] = \sum_{i=1}^{P_N} \frac{L_{N_i}^2}{R_N^2 P_N} \quad (23)$$

where  $P_N$  is the number of messages processed at node  $N$  in the signaling flow,  $n_E$  is the number of eNodeBs accommodated in the EPC,  $R_N$  is the amount of server resource of node  $N$  in terms of the number of statements that can be processed per unit time, and  $L_{N_i}$  is the number of the statements of the program involved in the processing of a  $i$ th signaling message at node  $N$ .

### C. Data Transmission Time

When the link speed between nodes  $N_1$  and  $N_2$  is  $W_{N_1, N_2}$  and the message size is  $C$ , a time  $t_{d_{N_1, N_2}}$  is required to transmit the message; this is derived by (24).

$$t_{d_{N_1, N_2}} = \frac{C}{W_{N_1, N_2}} \quad (24)$$

The data transmission time  $t_d$  is the sum of all data and signaling message transmissions and is derived as (25),

$$t_d = \sum_{N_1, N_2 \in \mathbb{V}} (n_{d_{N_1, N_2}} \cdot t_{d_{N_1, N_2}}) \quad (25)$$

where  $\mathbb{V}$  represents a set of nodes which transmit data and signaling messages and  $n_{d_{N_1, N_2}}$  is the number of data and signaling messages transmitted from  $N_1$  to  $N_2$ .

## IV. NUMERICAL EVALUATION

In this section, we present numerical evaluation results of the analysis in Section III.

### A. Parameter Settings

We set the parameters as follows:  $T_c = 20,000$  [slots],  $T_i = 10$  [s],  $B_M = 20$  [ms],  $n_M = 10$ ,  $P = 54$  (for LTE) / 48 (for NB-IoT), and  $B_A = 1$  [s].  $n_R$  is determined while we assume that the radio bandwidth of both LTE and NB-IoT is 20 [MHz] and NB-IoT is deployed In-band mode. The propagation delays of signaling messages and the link speed between EPC nodes are configured as follows (note that the propagation delays do not include the processing time for signaling messages).

- UE–eNodeB: 20 [ms], 22.8 [Mbps] (for LTE) / 0.106 [Mbps] (for NB-IoT)
- eNodeB–SGW/PGW: 7.5 [ms], 1000 [Mbps]
- eNodeB–MME: 10 [ms], 1000 [Mbps]
- SGW/PGW–MME: 10 [ms], 1000 [Mbps]

Note that the data rate of the link between UE and eNodeB is determined based on  $n_R$  and  $N_{RU}$ . The values of the resources of the EPC nodes are as follows.

- UE:  $1.5 \times 10^6$  [statements/s]
- eNodeB:  $3.0 \times 10^6$  [statements/s]
- MME:  $1.0 \times 10^7$ ,  $8.0 \times 10^7$  [statements/s]
- SGW/PGW:  $1.0 \times 10^7$ ,  $8.0 \times 10^7$  [statements/s]

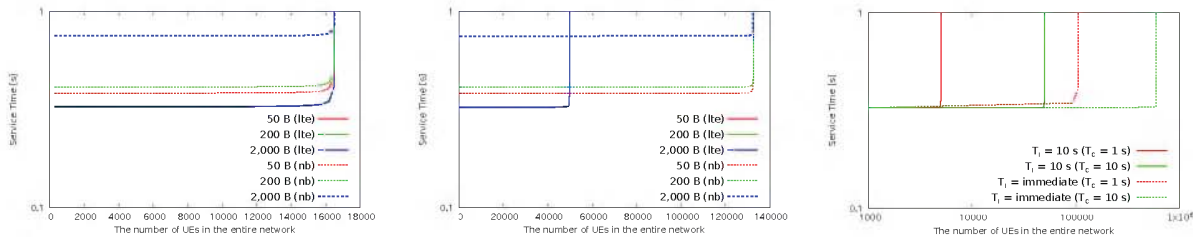
These parameter settings are based on the assumption that SGW and PGW are integrated into a single node, as in the state-of-the-art implementation design of EPC. We also assume that MME, HSS, and PCRF are virtualized and located in the cloud environment owned by the mobile network operator, whereas eNodeB and SGW/PGW are located in the transport network without virtualization.

### B. Results and Discussions

1) *Comparison of LTE and NB-IoT*: Fig. 4(a) and Fig. 4(b) present the service time  $t_{service}$  in (1) as a function of the number of accommodated UEs in the network. Fig. 4(a) is the case when the amount of server resources corresponding to MME and SGW/PGW is  $1.0 \times 10^7$  [statements/s], and Fig. 4(b) is for  $8.0 \times 10^7$  [statements/s]. In the figures, the numbers in the legend indicate the size of the data transmitted. (lte) indicates the results of LTE and (nb) is for NB-IoT. In both figures, we can observe that the service time becomes quite large when the number of UEs reaches a certain value. We consider that number as the number of UEs that can be accommodated with in the network. When the number of UEs is small, the processing time of signaling messages and the random access time are enough small to ignore. However, the propagation delays of signaling messages and the data transmission time do not depend on the number of accommodated UEs with in the network.

From Fig. 4(a), we can observe that LTE and NB-IoT networks can accommodate the same number of UEs. This results from the fact that the server resources of MME and SGW/PGW nodes are insufficient and these nodes are the bottleneck of the network. It is also shown that the service time of LTE is smaller than that of NB-IoT. This is because results from the fact that of the difference in the amount of allocated radio resource to each UE, 2/3 RBs for NB-IoT compared to 6 RBs in the case of LTE. This difference also results in an increased service time when increasing data size. In LTE, the service time remains almost unchanged for any data size to be transmitted, whereas it increases significantly in NB-IoT.

From Fig. 4(b), on the other hand, when the server resources of MME and SGW/PGW are increased, it is found that NB-IoT can accommodate more UEs than LTE because that the smaller amount of allocated radio resource for each UE in NB-IoT results in a larger number of UEs that are successfully



(a)  $1.0 \times 10^7$  [statements/s] for server resource (b)  $8.0 \times 10^7$  [statements/s] for server resource (c) Effect of immediate release of radio resources

Fig. 4: Evaluation results

allocated the radio resource concurrently. In other words, in Fig. 4(b), the radio access network is the bottleneck, as opposed to the condition in Fig. 4(a) where EPC nodes are the bottlenecks.

2) *Effect of immediate release of radio resources*: Fig. 4(c) shows the evaluation results of an LTE network when the data size is 2,000 [bytes] and the server resources of the EPC nodes are  $6.4 \times 10^8$  [statements/s]. In the figure,  $T_i$  indicates the value of the inactivity timer and  $T_i = \text{immediate}$  suggests results with immediate release of radio resources.  $T_c$  indicates the data transmission cycle of UEs. The figure shows that the immediate release of radio resources can significantly improve the network capacity because the holding time of the allocated radio resource decreases. In other words, the bottleneck of the network moves from the radio access network to the EPC nodes by introducing the immediate release of radio resources.

Moreover, the figure shows that the immediate release of radio resources with  $T_c = 1$  [s] is more effective than that with  $T_c = 10$  [s]. In detail, when  $T_c = 1$  [s], the number of UEs that can be accommodated in the network increases to 20.7 times, compared to 11.9 times for  $T_c = 10$  [s]. The reason of this is that the communication requests generated from UEs increases when  $T_c$  is small. Following this, the immediate release of radio resources can significantly increase the number of communication requests accommodated per unit time.

## V. CONCLUSION

In this paper, we presented mathematical analyses of the performance of mobile cellular networks that accommodate periodic C-IoT communications with immediate release of radio resources. We compared the performance of LTE and NB-IoT networks and demonstrated that the NB-IoT network can accommodate larger number of UEs than the LTE network, but gives the larger latency in data transmission. We also showed that the effect of the immediate release of radio resources is quite substantial for periodic C-IoT communications.

In future work, we plan to explore optimal parameter configurations of LTE and NB-IoT networks in accommodating periodic C-IoT communications, based on the analysis in this paper. Also, the evaluation of methods that reduce the overhead of bearer establishment procedure as in [14] is an important issue for effectively accommodating C-IoT

communications to mobile cellular networks. Additionally, we plan for experimental evaluation to support the results mentioned in this paper.

## ACKNOWLEDGMENT

This work was partially supported by Grant No. 19104 from the National Institute of Information and Communications Technology (NICT) in Japan.

## REFERENCES

- [1] 3GPP TS 45.820 V13.1.0, *Cellular System Support for Ultra-low Complexity and Low Throughput Internet of Things (CIoT)*. Dec. 2015.
- [2] A. ElNashar and M. El-saidny, *Practical Guide to LTE-A, VoLTE and IoT: Paving the way towards 5G*. Wiley, 2018.
- [3] 3GPP TR 36.300 V13.4.0, *Evolved Universal Terrestrial Radio Access (E-UTRA) and Evolved Universal Terrestrial Radio Access Network (E-UTRAN); Overall description; Stage 2*. June 2016.
- [4] B. Martínez, F. Adelantado, A. Bartoli, and X. Vilajosana, "Exploring the Performance Boundaries of NB-IoT," *CoRR*, vol. abs/1810.00847, 2018.
- [5] M. Lauridsen, I. Z. Kovacs, P. Mogensen, M. Sorensen, and S. Holst, "Coverage and Capacity Analysis of LTE-M and NB-IoT in a Rural Area," in *Proceedings of 2016 IEEE 84th Vehicular Technology Conference (VTC-Fall)*, pp. 1–5, Sept. 2016.
- [6] S. Persia and L. Rea, "Next Generation M2M Cellular Networks: LTE-MTC and NB-IoT Capacity Analysis for Smart Grids Applications," in *Proceedings of 2016 AEIT International Annual Conference (AEIT)*, pp. 1–6, Oct. 2016.
- [7] P. Andres-Maldonado, P. Ameigeiras, J. Prados-Garzon, J. J. Ramos-Muñoz, and J. M. López-Soler, "Optimized LTE Data Transmission Procedures for IoT: Device Side Energy Consumption Analysis," *CoRR*, vol. abs/1704.04929, 2017.
- [8] 3GPP TS 36.213 V15.7, *Physical layer procedures (Release 15)*. Sept. 2019.
- [9] O. Liberg, M. Sundberg, E. Wang, J. Bergman, and J. Sachs, *Cellular Internet of Things: Technologies, Standards, and Performance*. Elsevier Science, 2017.
- [10] M. Sauter, *From GSM to LTE-Advanced Pro and 5G: An Introduction to Mobile Networks and Mobile Broadband*. Wiley, 2017.
- [11] "OpenAirInterface." available at <http://www.openairinterface.org/>.
- [12] G. C. Madueno, J. J. Nielsen, D. M. Kim, N. K. Pratas, C. Stefanovic, and P. Popovski, "Assessment of LTE Wireless Access for Monitoring of Energy Distribution in the Smart Grid," *IEEE Journal on Selected Areas in Communications*, vol. 34, pp. 675–688, Mar. 2016.
- [13] J. Y. Cheah and J. M. Smith, "Generalized M/G/C/C State Dependent Queueing Models and Pedestrian Traffic Flows," *Queueing Systems*, vol. 15, pp. 365–386, 1994.
- [14] S. Abe, G. Hasegawa, and M. Murata, "Effects of C/U Plane Separation and Bearer Aggregation in Mobile Core Network," *IEEE Trans. Network and Service Management*, vol. 15, no. 2, pp. 611–624, 2018.
- [15] B. Avi-Itzhak and S. Halfin, "Expected Response Times in a Non-Symmetric Time Sharing Queue with a Limited Number of Service Positions," in *Proceedings of ITC-12*, pp. 1485–1493, 1988.